Short communication

Interfacial lithium-ion transfer at the LiMn$_2$O$_4$ thin film electrode/aqueous solution interface

N. Nakayama [a], T. Nozawa [a], Y. Iriyama [a], T. Abe [a], Z. Ogumi [a,*], K. Kikuchi [b]

[a] Department of Energy and Hydrocarbon Chemistry, Graduate School of Engineering, Kyoto University, Nishikyo-ku, Kyoto 615-8510, Japan
[b] Department of Materials Science, The University of Shiga Prefecture, Hikone, Shiga 552-8533, Japan

Available online 27 June 2007

Abstract

Interfacial lithium-ion transfer at the LiMn$_2$O$_4$ thin film electrode/aqueous solution was investigated. The cyclic voltammograms of the film electrode conducted in the aqueous solution was similar to an adsorption-type voltammogram of reversible system, suggesting that fast charge transfer reaction proceed in the aqueous solution system. We found that the activation energy for this interfacial lithium-ion transfer reaction obtains 23–25 kJ mol^{-1}, which is much smaller than that in the propylene carbonate solution (50 kJ mol^{-1}). This small activation energy will be responsible for the fast interfacial lithium-ion transfer reaction in the aqueous solution. These results suggest that fast lithium insertion/extraction reaction can be realized by decreasing the activation energy for interfacial lithium-ion transfer reaction.
© 2007 Elsevier B.V. All rights reserved.

Keywords: Interfacial lithium-ion transfer; LiMn$_2$O$_4$ thin film

1. Introduction

Rechargeable lithium-ion batteries (LIBs) have received much attention in recent years as a power source for hybrid or electric vehicles. However, there are some problems to address when applying this battery system in those large devices, such as power density, safety, and cost. In general, commercially available lithium-ion batteries use organic solvents in the electrolyte. This organic electrolyte is flammable and toxic, raising problems from the viewpoint of safety. Moreover, the use of organic solvents can seriously slow charge transfer, in this case interfacial lithium-ion transfer, and hence the reaction rate at the electrode/electrolyte interface, leading to a decrease in power density [1–3].

One effective method for overcoming these problems will be to replace the organic electrolytes with aqueous solution. The idea of using aqueous solution as the electrolyte in LIBs was first reported by Dahn and co-workers [4]. It is true that LIBs using aqueous solution cannot operate at high voltage, but such systems are safe and inexpensive, have a low environmental load, and the lithium-ion conductivity is very high. In addition, Lee and Pyun have pointed out that charge transfer resistance occurring in aqueous solution system becomes very small. They suggested this reason that resistive surface film is not formed on the electrode surface in aqueous solution system and then charge transfer reaction is not impeded by the surface film unlike the case of organic electrolyte system [5]. Our group has focused on the kinetics of interfacial lithium-ion transfer reaction at the electrode/electrolyte interface and found that there is large activation energy for interfacial lithium-ion transfer process at conventional organic electrolyte/electrode interface [6–10]. Moreover, this large activation energy has been clearly observed even in the interfacial lithium-ion transfer process at conventional organic electrolyte/inorganic solid electrolyte interface, where such resistive surface film will not be expected on the solid electrolyte surface [3]. From these results, it will be considerable that smaller interfacial lithium-ion transfer resistance observed in aqueous solution are originated from other factors. Although some researchers have reported on the aqueous lithium-ion battery system [4,5,11], few studies have focused on these kinetic aspects of the interfacial lithium-ion transfer reaction at the electrode/aqueous solution [5].

Spinel-structured LiMn$_2$O$_4$ has a three-dimensional framework. Lithium ions are electrochemically removed from tetrahedral 8a sites in the anodic reaction, and they can be reinserted into the same sites in the cathodic reaction over the compositional range $0 \leq x \leq 1$ in Li$_x$Mn$_2$O$_4$. This unique structure prevents the insertion of a hydroxyl group in the framework.

Moreover, this material has remarkable selectivity for lithium ions, and can display lithium-ion sieve properties [12]. Although the Li^+–H^+ ion-exchange reaction has been reported by several authors [13–16], these reactions usually occur at lower pH (acidic) conditions. According to the reported Pourbaix diagram [17], it is expected that the lithium insertion/extraction reaction of $LiMn_2O_4$ can operate stably also in aqueous solution in appropriate pH range.

Based on the above concept, we investigated the kinetics of interfacial lithium-ion transfer at the $LiMn_2O_4$ thin film electrode/aqueous solution. Thin film electrodes have several advantages over composite electrodes for investigating interfacial reactions. They are thin, flat, and free from impurities, such as conductive additives and acetylene black, and can provide a uniform potential distribution in the electrode. We have already fabricated $LiMn_2O_4$ thin film electrodes by pulsed laser deposition and reported their electrochemical lithium insertion/extraction reactions in conventional organic electrolytes [10]. The results shown here are discussed in comparison with those results.

2. Experimental

2.1. Preparation of LiMn2O4 thin films by pulsed laser deposition

Highly crystalline $LiMn_2O_4$ thin films with ca. 60 nm in thickness were prepared by pulsed laser deposition. PLD was conducted in a vacuum chamber made of stainless steel. A KrF excimer laser (248 nm, Japan Storage Batteries, Model EXL-210) was used as a light source. The laser beam was focused on the target at an incident angle of 45°. The energy density of the beam was fixed at 1.4 J cm^{-2}, which was measured with a joule meter (Gentec, EC-500), with a repetition frequency of 10 Hz. The base pressure of the vacuum chamber was $<5 \times 10^{-3}$ Pa. Oxygen gas was introduced into the chamber and the pressure was maintained at 23 Pa during deposition. Thin films of $LiMn_2O_4$ were deposited on quartz glass covered with Pt film prepared by RF sputtering and the deposited area was 0.07 cm^2. The substrate temperature was maintained at 973 K during the deposition and the deposition time was 1 h. The distance between the target and substrate was kept at 50 mm. The resultant films were characterized by XRD, and both the total mass and the Li/Mn ratio of the deposited thin films were analyzed by ICP-AES.

2.2. Cyclic voltammetry measurement of the LiMn2O4 thin films

Electrochemical lithium insertion/extraction reactions of the $LiMn_2O_4$ thin films were investigated by cyclic voltammetry. Electrochemical measurements were carried out using three-electrode cells. The counter and reference electrodes were platinized platinum mesh electrode and a NaCl-saturated Ag/AgCl electrode, respectively. The aqueous solution used in this study was $LiNO_3$ or $LiCF_3SO_3$ dissolved in ultra-pure water. The three-electrode cell was sealed in a glass case and

the electrochemical measurements were conducted in it at room temperature. Measurements were also conducted in 1 mol dm^{-3} $LiClO_4$ dissolved in propylene carbonate (PC) solution using three-electrodes cell which had same configuration with the above aqueous solution system. In those electrochemical measurements, same lithium metal foils were used as both reference and counter electrodes, and the measurements were performed in an argon-filled glove box at room temperature.

2.3. Measurement of interfacial lithium-ion transfer resistance at the LiMn2O4 thin film electrode/electrolyte interface

Interfacial lithium-ion transfer resistance at $LiMn_2O_4$/aqueous solution was investigated by AC impedance spectroscopy. The electrode potential was kept at a given potential until the residual current decreased down to 0.1 μA. After the cell attained equilibrium, the AC impedance measurement was carried out at that potential. The impedance was measured by applying a sine wave of 5 mV (rms) amplitude over the frequency range of 100 kHz to 10 mHz. This measurement was conducted over the temperature range of 278–323 K. These measurements were also conducted on the cell employing organic electrolyte.

3. Results and discussions

3.1. Characterization of LiMn2O4 thin films

Fig. 1 shows an XRD pattern of the thin film deposited on a quartz glass covered with a Ti/Pt thin film. Diffraction peaks assigned to spinel-structured $LiMn_2O_4$ were clearly observed [18]. Broad diffraction peaks at around 20° were from the quartz glass substrate, and the peaks observed at 39.7, 46.2, and 67.5°
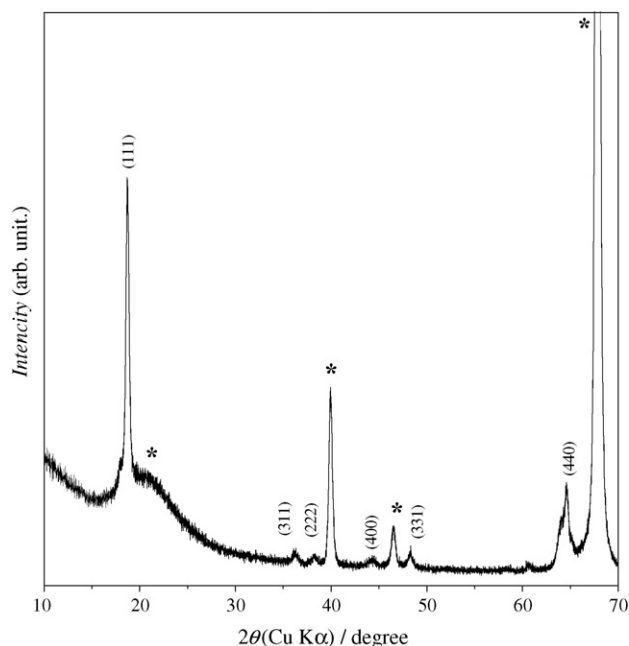

Fig. 1. XRD pattern of $LiMn_2O_4$ thin film deposited on platinum sheet. Peaks marked by asterisk (*) are from the substrate.
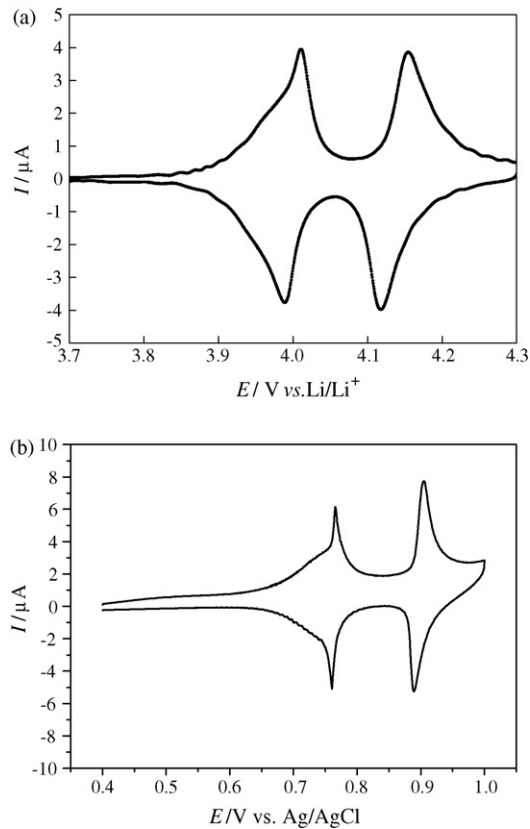
Fig. 2. Cyclic voltammograms of LiMn$_2$O$_4$ thin films in (a) 1 mol dm^{-3} LiClO$_4$-PC and (b) 1 mol dm^{-3} LiNO$_3$-H$_2$O ($v = 1$ mV s^{-1}).

were from the Pt film. Measurement by ICP-AES revealed that the Li/Mn ratio in the thin film was 0.48. These results reveal that the prepared thin films are highly crystalline and nearly stoichiometric spinel-structured LiMn$_2$O$_4$.

3.2. Cyclic voltammetry measurement of LiMn$_2$O$_4$ thin films

Fig. 2(a and b) show cyclic voltammograms at third cycle of LiMn$_2$O$_4$ thin films in 1 mol dm^{-3} LiClO$_4$-PC and in 1 mol dm^{-3} LiNO$_3$-H$_2$O, respectively. In Fig. 2(a), two coupled current peaks were observed at 4.0 and 4.135 V in E_{eq} (vs. Li/Li$^+$). These are in good agreement with the previous report, and these peaks are due to the phase transition of LiMn$_2$O$_4$ during its lithium-ion insertion/extraction reaction [19]. The shape of the voltammogram in Fig. 2(b) is identical to Fig. 2(a), and the two coupled current peaks were observed at 0.763 and 0.898 V in E_{eq} (vs. Ag/AgCl). The potential difference between these two peaks consisted with that observed in organic electrolyte system. These results indicate that the electrochemical lithium-ion insertion/extraction reaction in these LiMn$_2$O$_4$ thin film electrodes occur in aqueous solution as with the case of the organic electrolyte system. Stable voltammograms were obtained for the repetition of the cycles in both cases.

We focused on the current peaks at the lower potential in the CVs, and both the peak currents and the peak potentials were
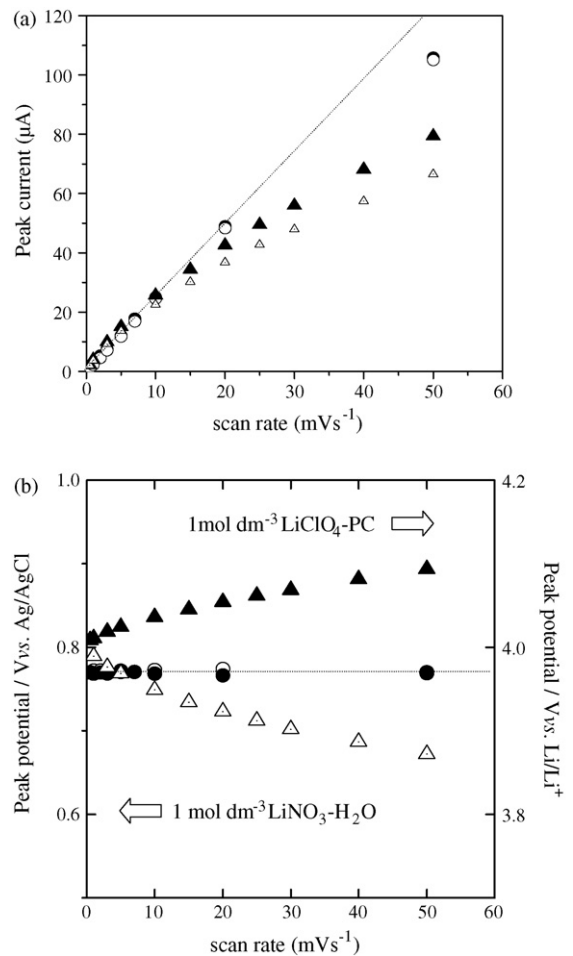

Fig. 3. Variation of (a) the current peaks and (b) the peak potential at the lower potential in Fig. 2 against potential sweep rates. Data shown by circles are from 1 mol dm^{-3} LiNO$_3$-H$_2$O and those by triangles are from 1 mol dm^{-3} LiClO$_4$-PC. The closed points are from anodic reaction and the open ones are from cathodic reaction.

plotted against potential sweep rates. Fig. 3(a) shows the relationship between the current peaks and potential sweep rates. Also, Fig. 3(b) shows the variation of peak potentials against potential sweep rates. As shown in Fig. 3(a), both the anodic and cathodic current peaks tended to increase in direct proportion to the potential sweep rate, which continued above at least 20 mV s^{-1} in the case of the aqueous solution system. It should be noted that the peak potential did not change in this potential sweep region, as shown in Fig. 3(b), and the peak separation between the anodic and cathodic current peak (ΔE_{pk}) was or less 10 mV. On the other hand, in the case of the organic electrolyte system, the peak current increased in proportion with potential sweep rates below 10 mV s^{-1}, but this proportionality deviated from a straight line after that. In addition, the ΔE_{pk} varied with the potential sweep rate as shown in Fig. 3(b).

Li and co-workers fabricated nanostructured LiMn$_2$O$_4$ electrodes consisting of LiMn$_2$O$_4$ nanotubules and investigated the ΔE_{pk} for the lower pontential reaction against potetntial sweep rates in aqueous solution system [11]. The ΔE_{pk} showed very small value (ca. 10 mV) in case of fine samples at low scan rate

(0.3 mV), while the ΔE_{pk} increased with the increase of potential sweep rates. As compared with their results, our film electrodes observed in aqueous solution maintained the initial ΔE_{pk} value even in higher potential sweep rates. As will be described later, the charge transfer reaction in this aqueous solution system proceeds very fast. Therefore, the different situation of the ΔE_{pk} against potential sweep rates will be ascribed to the difference in geometry of electrode.

When a current peak increases in direct proportion to the potential sweep rate, this voltammogram is generally recognized as a nondiffusion (adsorption)-type voltammogram [20]. This voltammogram is typically observed when the concentration of the redox species at the electrode surface is consistent with that of the bulk solution, and then the effects of mass transfer of the redox species on the electrode reaction can be neglected. In addition, in the case of reversible reaction systems, the charge transfer reaction proceeds much faster than the mass transfer reaction, and the ΔE_{pk} becomes 0 in ideal case regardless with the potential sweep rates. Although redox peaks in the voltammogram of this aqueous solution system remain small peak separation (10 mV) as shown in Fig. 3(b), this is probably because this reaction does not occur only on the electrode surface and reaction current due to the lithium-ion diffusion into the electrode mainly correspond to the peak current. However, because the film electrodes are very thin, lithium-ions in the film electrodes will be able to achieve equilibrium rapidly and then the diffusion of lithium ions in the film electrode will not be the rate-determining step at these scan rates. This prospect can be supported from the result that the I_p did not increase in proportion to the square root of the potential sweep rate in both cases.

It will be reasonable to expect that the lithium-ion diffusion itself in the film electrodes proceeds in the same manner in both cases, and then the differences shown in Fig. 3(a and b) do not originate from the diffusion of lithium-ion in the film electrode. Of course, conductivities in these solutions are different, and electrolyte resistance of organic electrolyte is larger than that of aqueous solution as shown in later AC impedance spectra. But the estimated iR drop in organic electrolyte was smaller than ΔE_{pk}; for example iR drop at $v = 30$ mV s^{-1} is roughly calculated to be 15 mV, which is much smaller than the value of ΔE_{pk} at this potential sweep rate ($\Delta E_{pk} = 167$ mV). These results suggest that the differences of electrode reaction properties shown in Fig. 3(a and b) are ascribed to the interfacial lithium-ion transfer reaction rates in both cases.

3.3. Interfacial lithium-ion transfer reaction at the LiMn₂O₄ thin film/aqueous solution interface

Fig. 4(a and b) show the Cole–Cole plots of LiMn$_2$O$_4$ thin films in organic electrolyte and in aqueous solution, respectively. Because the electrode potentials are different from each other; these data were obtained at nearly the same lithium-ion composition in LiMn$_2$O$_4$, that is, at 3.95 V for the organic electrolyte system and at 0.75 V for the aqueous system. Both spectra are composed of a semicircular arc in the high frequency region, followed by a vertical line to the real axis. The Warburg impedance
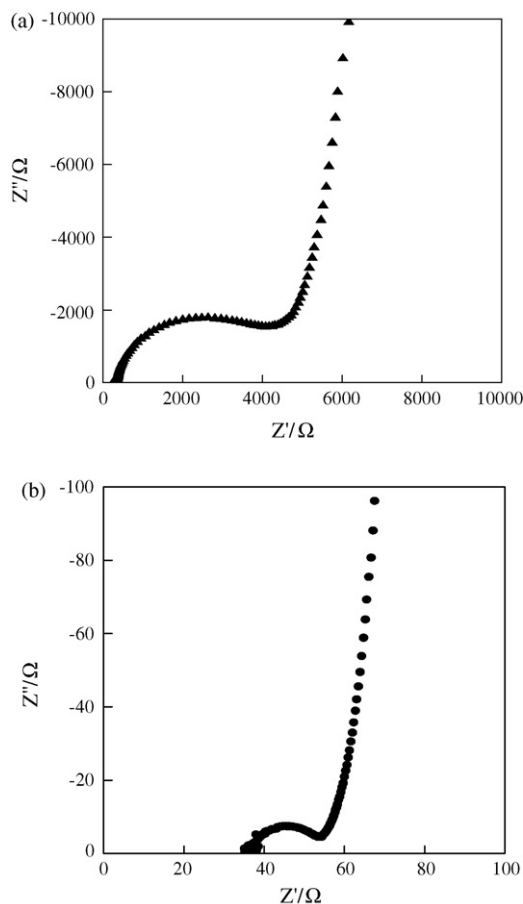

Fig. 4. Cole–Cole plots of interfacial lithium-ion transfer reaction at (a) LiMn$_2$O$_4$ thin film/1 mol dm^{-3} LiClO$_4$-PC at 3.95 V (vs. Li/Li$^+$) and (b) LiMn$_2$O$_4$ thin film/1 mol dm^{-3} LiNO$_3$-H$_2$O at 0.75 V (vs. Ag/AgCl).

corresponding to semi-infinite diffusion was not observed in either plot, indicating that the lithium-ion diffusion reaction into the thin film electrode proceeds quickly. These semicircular arcs are assigned to the interfacial lithium-ion transfer reaction at the LiMn$_2$O$_4$ thin film electrode/electrolyte interface. The interfacial lithium-ion transfer resistance estimated from the diameter of the semicircular arcs was 4000 Ω in the organic electrolyte system, and that valued only 20 Ω in the aqueous solution system. This drastic decrease observed in aqueous solution is identical to results reported by Lee and Pyun [5].

The temperature dependence of the interfacial lithium-ion transfer resistances was measured to investigate the kinetic aspects of these interfacial lithium-ion transfer reactions. The Arrhenius plots of reciprocal charge transfer resistance multiplied by absolute temperature against reciprocal temperature are shown in Fig. 5. These data were fitted to straight lines in every case, indicating that the reciprocal charge transfer resistance multiplied by absolute temperature can be expressed as follows:

$$\frac{T}{R_{ct}} = A \exp\left(-\frac{E_a}{RT}\right)$$

where E_a is the activation energy, T the absolute temperature, R the gas constant, R_{ct} the interfacial lithium-ion transfer
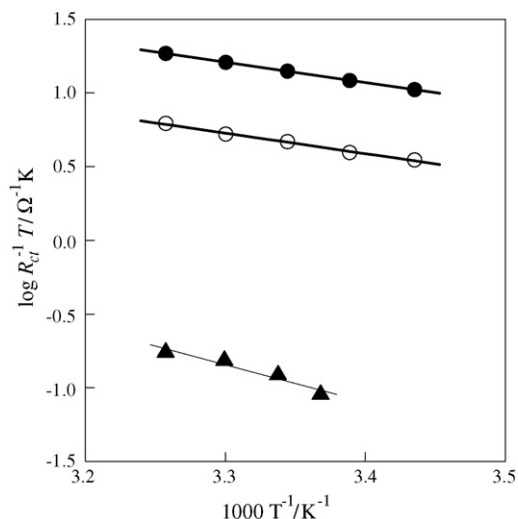
Fig. 5. Temperature dependency for interfacial lithium-ion transfer resistance of $LiMn_2O_4$ thin film in (●) 1 mol dm^{-3} $LiCF_3SO_3$-H_2O, (○) 0.1 mol dm^{-3} $LiCF_3SO_3$-H_2O, and (▲) 1 mol dm^{-3} $LiClO_4$-PC.

resistance, and *A* the pre-exponential factor. According to the above equation, the activation energy was measured in 1 and 0.1 mol dm^{-3} $LiNO_3$ aqueous solutions and the values were calculated to be 24 kJ mol^{-1} in both cases. The R_{ct} in 1 mol dm^{-3} $LiNO_3$ aqueous solution was smaller than that in 0.1 mol dm^{-3} one, which is probably because of the difference of lithium-ion activity in the solutions. On the other hand, the activation energy was valued at 50 kJ mol^{-1} in the case of organic electrolyte system, which is in good agreement with our previous work [10]. The activation energy was also measured in the aqueous solutions dissolving $LiCF_3SO_3$ at the same concentrations, and the results are summarized in Table 1. The activation energy gave nearly the same values even when the salt was changed from $LiNO_3$ to $LiCF_3SO_3$. These results strongly suggest that this activation energy depends on the interaction of lithium ions with water molecules.

Smaller activation energy observed in aqueous solution indicates that fast interfacial lithium transfer reaction proceeds at the $LiMn_2O_4$ thin film electrode/aqueous solution interface. In our previous study on the interfacial lithium-ion transfer reaction at the lithium ion conductive solid electrolyte/organic electrolyte interface, there is large activation energy for the reaction process at the electrode/organic electrolyte interface, and the activation energies strongly depended on the solvent species [3]. The difference in the activation energies between solvents was in good agreement with the difference in the reaction enthalpies

(Li^+ + single solvent = Li^+-single solvent). From these results, we concluded that the interfacial lithium-ion transfer reaction through the solid electrolyte/organic electrolyte interface is strongly affected by the desolvation process. We have already checked that this idea can be applied also to electrode/organic electrolyte interface where surface resistive film can be formed on the electrode surface [6–10]. The hydration enthalpy of lithium ions has been calculated to be -142 ± 8 kJ mol^{-1} [21], which is much smaller than the calculated reaction enthalpy of a single PC molecule with lithium-ion (-217.8 kJ mol^{-1}) [3]. Thus, the smaller activation energy measured in the aqueous solution system seems to be explained qualitatively by its smaller reaction enthalpy. However, the difference in the reaction enthalpies is much larger than that of the activation energies, indicating that we cannot simply apply the above idea for the aqueous solution system. Details of the reaction mechanism could not be elucidated only from this work, but we speculate that most considerable reason will be the difference of the transition state for the desolvation process in the aqueous solution system probably because of its small molecular size of water compared with the organic molecule. Of course, the difference in the ground state for the interfacial lithium-ion transfer reaction should also be considered. These are currently under investigation, which will be reported elsewhere in the near future.

4. Conclusions

The interfacial lithium-ion transfer reaction at the $LiMn_2O_4$ thin film electrode/aqueous solution interface was investigated and the results were compared with the conventional organic electrolyte system. Aqueous solution systems can largely decrease the reaction resistance in comparison with the propylene carbonate (organic) electrolyte system, which is in good agreement with previous reports.

We found that the activation energy for the interfacial lithium-ion transfer reaction in aqueous solution markedly decreases down to 23–25 kJ mol^{-1}, and does not tend to be affected by either the anion species or the lithium-ion activity in the solution. This small activation energy will enhance the interfacial lithium-ion transfer reaction rate, which permits a fast charge transfer reaction rate. The cyclic voltammograms observed in the aqueous solution was similar to an adsorption-type voltammogram of reversible system. Also, these results support the idea that fast lithium-ion insertion/extraction reaction can be realized by decreasing the activation energy for interfacial lithium-ion transfer reaction.

Table 1
Summaries of activation energies for interfacial lithium-ion transfer reaction in different kinds of aqueous solution

Salt species	Concentration (mol dm^{-3})	E_a (kJ mol^{-1})
$LiNO_3$	0.1	24
	1.0	24
$LiCF_3SO_3$	0.1	25
	1.0	23

References

[1] J. Vetter, P. Novák, M.R. Wagner, C. Veit, K.-C. Möller, J.O. Besenhard, M. Winter, M. Wohlfahrt-Mehrens, C. Vogler, A. Hammouche, J. Power Sources 147 (2005) 269.

[2] D.P. Abraham, R.D. Twesten, M. Balasubraminian, J. Kropf, D. Fischer, J. McBreen, I. Petrov, K. Amine, J. Electrochem. Soc. 150 (2003) 1450.

[3] T. Abe, F. Sagane, T. Ohtsuka, Y. Iriyama, Z. Ogumi, J. Electrochem. Soc. 152 (2005) 2151.

[4] W. Li, J.R. Dahn, D.S. Wainwright, Science 264 (1994) 1115.

[5] J.-W. Lee, S.-I. Pyun, Electrochim. Acta 49 (2004) 753.

[6] T. Abe, H. Fukuda, Y. Iriyama, Z. Ogumi, J. Electrochem. Soc. 151 (2004) A1120.

[7] Z. Ogumi, T. Abe, T. Fukutsuka, S. Yamate, Y. Iriyama, J. Power Sources 127 (2004) 72.

[8] T. Doi, K. Miyatake, Y. Iriyama, T. Abe, Z. Ogumi, T. Nishizawa, Carbon 42 (2004) 3183.

[9] Y. Iriyama, H. Kurita, I. Yamada, T. Abe, Z. Ogumi, J. Power Sources 137 (2004) 111.

[10] I. Yamada, T. Abe, Y. Iriyama, Z. Ogumi, Electrochem. Commun. 5 (2003) 502.

[11] N. Li, C.J. Patrissi, G. Che, C.R. Martin, J. Electrochem. Soc. 147 (2000) 2044.

[12] K. Ooi, Y. Miyai, S. Kanoh, Solvent Extr. Ion Exch. 5 (1987) 561.

[13] X.-M. Shen, A. Clearfield, J. Solid State Chem. 64 (1986) 270.

[14] Q. Feng, Y. Miyai, H. Kanoh, K. Ooi, Langmuir 8 (1992) 1861.

[15] B. Ammundsen, P.B. Aitchison, G.R. Burns, D.J. Jones, J. Rozière, Solid State Ionics 97 (1997) 269.

[16] B. Ammundsen, J. Rozière, M.S. Islam, J. Phys. Chem. B 101 (1997) 8156.

[17] Y. Kanzaki, A. Taniguchi, M. Abe, J. Electrochem. Soc. 138 (1) (1991) 333.

[18] JCPDS No. 38-0789.

[19] T. Ohzuku, M. Kitagawa, T. Hirai, J. Electrochem. Soc. 137 (1990) 769.

[20] A.J. Bard, L.R. Faulkner (Eds.), Electrochemical Methods—Fundamental and Applications, second ed., Wiley, USA, 2000.

[21] J.E. Del Bene, H.D. Mettee, M.J. Frisch, B.T. Luke, J.A. Pople, J. Phys. Chem. 87 (1983) 3279.